Research Article | Vol. 28, No. 12 / 8 June 2020 / Optics Express 17773

Optics EXPRESS

Observation of four Fermi-Pasta-Ulam-Tsingou recurrences in an ultra-low-loss optical fiber

GUILLAUME VANDERHAEGEN,[1] PASCAL SZRIFTGISER,[1] ALEXANDRE KUDLINSKI,[1] MATTEO CONFORTI,[1] STEFANO TRILLO,[2] MAXIME DROQUES,[3] AND ARNAUD MUSSOT[1,4,*]

[1] *Univ. Lille, CNRS, UMR 8523-PhLAM – Physique des Lasers Atomes et Molécules, F-59000 Lille, France*
[2] *Department of Engineering, University of Ferrara, Via Saragat 1, 44122 Ferrara, Italy*
[3] *Alcatel Submarine Networks, 950, Quai de la Loire, 62225 Calais Cedex, France*
[4] *Institut Universitaire de France (IUF), France*
[*] *arnaud.mussot@univ-lille.fr*

Abstract: We report the experimental observation of more than four Fermi-Pasta-Ulam-Tsingou recurrences in an optical fiber thanks to an ultra-low loss optical fiber and to an active loss compensation system. We observe both regular (in-phase) and symmetry-broken (phase-shifted) recurrences, triggered by the input phase. Experimental results are confirmed by numerical simulations.

1. Introduction

The Fermi-Pasta-Ulam-Tsingou (FPUT) recurrence process describes the ability of a strongly multimodal nonlinear system to come back to its initial state after the (potentially complex) redistribution of modal energies, as discovered by Fermi and co-workers in the 50s by numerically modelling nonlinear chains of oscillators [1]. Several recurrences can occur before the system exhibits the tendency to evolve towards a thermalized state ultimately characterized by the equipartition of the energy between all the modes. Parametric conversion and in particular seeded modulational instability (MI) in focusing cubic media offers the possibility to investigate experimentally FPUT recurrence, as demonstrated in hydrodynamics [2] and optics, both in fibers [3–7] and in the spatial domain in bulk crystals [8]. In this case the hallmark of FPUT recurrence is the return of Fourier modes to their input amplitude and relative phase after the growth into a triangular frequency comb (this is distinct from other mechanisms of recurrence due to multi-soliton fission, characteristic for example of regimes described by the weakly dispersing Korteweg-de Vries model [9–11]). In the context of the FPUT phenomenon, a major issue is to investigate and understand the transition from the recurrent regime to the thermalized state. Such transition usually requires very long times in weakly nonlinear FPUT chains [12]. However, it is expected to be relatively fast when driven by MI in the presence of noise, as ruled by the nonlinear Schrödinger equation [13]. Nevertheless, an essential prerequisite for such studies becomes the ability to extend the detection to the regime of several recurrences beyond the current limit of two or three recurrences, as reported recently in fibers [5–7] or bulk [8], respectively.

Fiber optics constitute a fantastic test bed to perform FPUT experiments since they offer an easy tuning of initial conditions and a precise control of fiber parameters. However, the attenuation, though very low in modern optical fibers with a recent record of 0.1424 dB/km [14], constitutes the main limitation of such waveguides to investigate FPUT process because even very weak losses prevent the appearance of several recurrences. In standard fiber optics systems, the observation of more than a single recurrence has been critical due to this limitation [3,4,6]. Recently, we reported the observation of two recurrences [5] thanks to an active compensation of the loss using a counter-propagating Raman pump. A different group took benefit of a recirculating loop to also record a limit of two recurrences [7]. Reaching two recurrence cycles

#391560 https://doi.org/10.1364/OE.391560
Journal © 2020 Received 26 Feb 2020; revised 17 May 2020; accepted 18 May 2020; published 29 May 2020

Optics EXPRESS

has a been a qualitative major advance since it allowed to explore, on one hand, the rich dynamics of these nonlinear systems through the observation of the intrinsic symmetry breaking nature of FPUT [5] and, on the other hand, the invariance of the nonlinear spectrum of the system in the inverse scattering sense [7]. Nonetheless, much remains to be done, since at present it is not clear how far one can go in observing a higher number of recurrences, which is preparatory for further studies on the onset of thermalization.

In this work, we make a step further in this direction by reporting for the first time the observation of more than four recurrences by exploiting an ultra-low loss optical fiber developed for ultra-long-haul submarine telecommunication systems [14]. More specifically, our aim is to further show that the four recurrences manifest themselves according to the two distinct types of possible evolutions without exhibiting cross-over over the whole fiber length. The two evolution scenarios are determined solely by the input relative phase of the MI sidebands and are characterized by successive shifted versus unshifted temporal patterns at the points of maximum compression, respectively [5]. To this end, using an ultra-low loss optical fiber appears the most natural choice since it is known from the numerics [15] and experiments [16] that too large linear losses have the detrimental effect to induce all evolutions to become of the shifted type, regardless of the initial condition. Nevertheless, due to the long fiber span considered here, even the residual ultra-low losses are critical thereby requiring adequate compensation. As a result, the use of such ultra-low loss fiber has required to considerably improve our setup as described below.

2. Experimental setup

We basically exploited the same vector heterodyne optical time domain reflectometer (HOTDR) system described in details in Ref. [5]. The experimental setup is sketched in Fig. 1. In this paper, for the sake of simplicity, we will only provide a short description of the HOTDR system. In particular, we will only focus on the modifications required to improve its performances in order to be able to record these four recurrences. A 1550 nm CW laser signal is intensity modulated to get 50 ns duration square shaped pulses with a repetition rate of 4.9 kHz (see the inset in the right-bottom of Fig. 1). It is then phase modulated and filtered to create a strong pump surrounded by two weak symmetric sidebands (idler and signal waves) whose relative phases can be tuned thanks to a commercial complex optical filter (Waveshaper, Finisar). These are injected into the ultra-low loss optical fiber (ULLF) of 18.35 km length. The amplitude and phase evolution of the three frequencies (pump and sidebands) along the fiber are recorded thanks to the Rayleigh backscattered light via a multiple heterodyne detection system (beating with a multi-lines local oscillator). The group velocity dispersion of the ULLF is $\beta_2 = -24\times10^{-27}$ s^2/m and the nonlinear coefficient is $\gamma = 0.77$/W/km. The pump power is set to P = 840 mW and the signal/idler to pump ratio is −10 dB. The frequency shift from the pump is set to f = 34 GHz, very close to the peak MI gain frequency (f_{peak}=37 GHz from spontaneous MI spectrum, in agreement with well known expression $f_{peak}=[\gamma P/(2\,\pi^2 \mid \beta_2 \mid)]^{1/2}$). The original HOTDR system performances were reported by using a standard SMF28 fiber which did not allow to record more than two recurrences [5]. Thus we had to improve its performances to generate and observe more. The main modifications of the original HOTDR system are the following: we used (i) an ultra-low loss fiber and (ii) an optimized Raman pumping scheme to actively compensate the losses. The ULL is a commercial fiber (Corning Vascade EX2000 fiber) with 0.147 dB/km. This very low loss value is very close to the record of 0.1419 dB/km obtained for non-commercial fiber [14]. This impressive performance is due to a lowering of the microscopic glass network structure disorder by using Ge-free silica core included fluorine co-doping. However, such a fiber has a lower nonlinear coefficient than the one of the SMF28 used in Ref. [5]. Consequently, we add to increase the pump power to get similar nonlinear lengths, as detailed above. A higher amplification at the input by EDFA1 (Fig. 1) induces an important degradation of the signal

Optics EXPRESS

to noise ratio of the signal launched inside the fiber. This degradation prevented the recording of clean back reflected traces. This problem was circumvented by adding a booster just before the intensity modulator (SOA in Fig. 1). The amplification by EDFA1 can then be reduced and the intensity modulator combined with the Waveshaper cut significantly the background noise amplified by the booster. In our experimental system, the fiber length is more than two times the length of the one used in Ref. [5] (18.35 km vs 7.7 km). The repetition rate of the signals launched inside the fiber was reduced from 9.8 kHz to 4.9 kHz to prevent the temporal overlap between two consecutive back-reflected OTDR traces. One OTDR trace has a duration of 179 µs corresponding to one round-trip within the fiber which is shorter than the period of the signal launched in the fiber (1/4.9 kHz = 204 µs). Concerning the Raman pump used to get an active compensation of the loss, in these new experiments, we implemented a Raman pump located at 1450 nm (against 1480 nm in Ref. [5]) to take benefit of the maximum Raman gain on the signal to be amplified located at 1550 nm (13.2 THz away).

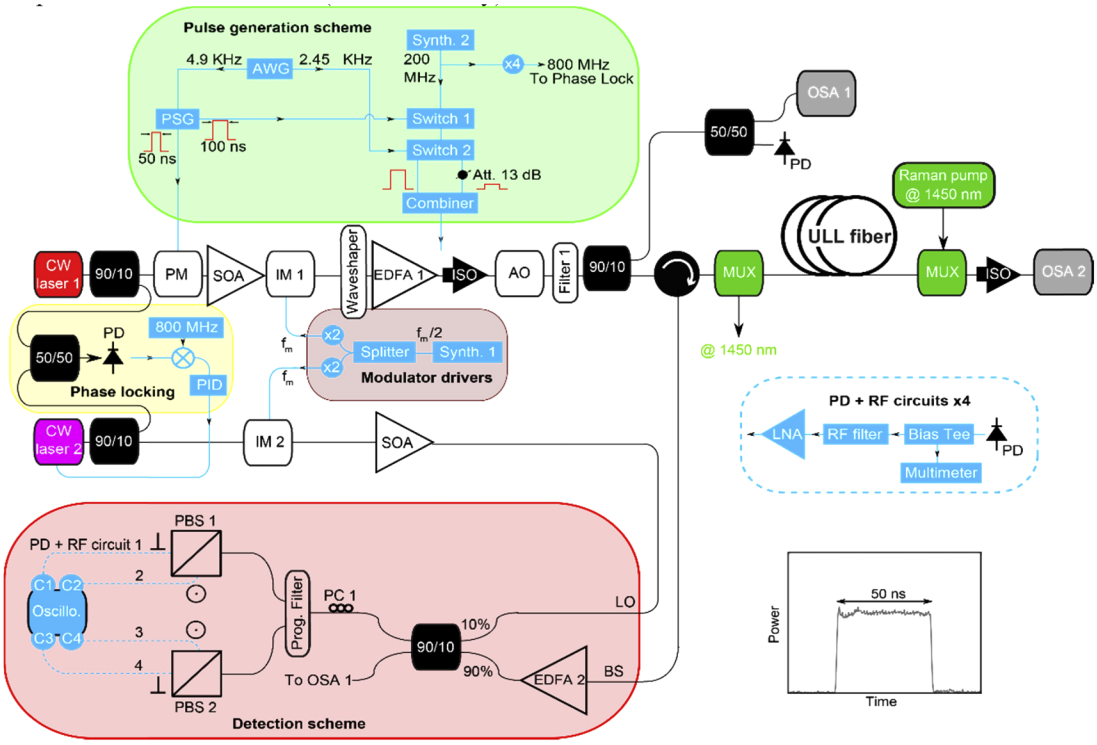

Fig. 1. Experimental setup. Laser 1 is a narrow linewidth (100 Hz at FWHM) CW laser and laser 2 is a continuous distributed feedback laser diode. IM(1,2): intensity modulator, PM: phase modulator, AWG: arbitrary waveform generator, EDFA(1,2): erbium-doped fibre amplifier, ISO: isolator, AO: acousto-optic modulator, MUX: multiplexer or de-multiplexer, SOA : semiconductor optical amplifier, PID: proportional, integral, derivative controller, PD: photo-detector, PC: polarization controller, PBS: polarisation beam splitter, RF: radio frequency, LNA: low-noise radio frequency amplifier, ULL : ultra-low loss fiber. All the instruments of the setup (including the oscilloscope) are referenced to the same 10 MHz clock. Inset: temporal shape of the pulses launched inside the fiber.

Hence, these improvements allowed us to achieve a quasi-transparent optical fiber of 18.35 km length, corresponding to about 10 nonlinear lengths ($L_{NL}=(\gamma P)^{-1}=1546$ m) which is remarkable in a quasi-purely conservative system. We further estimate that, due to Raman pump depletion

Optics EXPRESS

and losses, the total power experiences along the fiber a maximum variation of 10% around its initial value.

3. Results/discussion

In the following, we report the observation of the two types of recurrences that can arise in a FPUT system as long as more than two recurrences can be observed [17–19]. Here a single cycle of recurrence is intended as the evolution of the modulated input into the stage of maximally amplified sidebands (or maximally compressed pulse train in time domain) followed by the return to a minimum of the modulation (sidebands). We remind that the two possible types of dynamics involve either regular or symmetry-broken recurrences, with the difference between the two becoming mostly evident with reference to spatio-temporal evolution portraits. Indeed, either successive maximum compression points can occur in phase (regular recurrences) or π-phase shifted (symmetry broken recurrences). Incidentally, we emphasize that evolutions with π-phase shift are correctly defined as recurrences with broken symmetry, as they correspond to the equivalent motion of a particle in a double-well or Mexican hat potential characteristic of any symmetry breaking process [5]. However, they can be regarded as more natural in the sense that they are the continuation of the Fourier mode evolution dominated by the dispersion [20]. Conversely, regular recurrences are more exotic in the sense that they are uniquely produced by the onset of MI and are intrinsically associated to the phase-space deformation induced by this nonlinear effect [20].

To get a global overview of the system, it is convenient to plot the evolution of the signal power and phase in a phase plane ($\eta\cos(\Delta\Phi)$, $\eta\sin(\Delta\Phi)$), where $\Delta\Phi$ is the relative phase between the pump, signal and idler waves, defined as $\Delta\Phi = ½\,(2\varphi_{pump} - \varphi_{signal} - \varphi_{idler})$, $\eta(\zeta)$ the signal power normalized to the total power, ζ being the generic distance along the fiber [5,17]. In such phase plane, regular recurrences correspond to trajectories confined within the right (or left) semi-plane while those with broken symmetry span the whole plane [5,17,21]. They are separated by a homoclinic loop or separatrix (the Akhmediev breather), being internal or external to the latter, respectively [5,17,19,20,22]. In a lossless system, it is possible to address one type of recurrence or the other by controlling the initial conditions. Note that, experimentally, it is more convenient to keep constant the initial amplitude of the sidebands and to change the initial phase value $\Delta\Phi_{init} = \Phi(0)$ rather than tuning the power of the perturbation. Indeed, switching from inner to outer trajectories at a fixed phase may require sidebands with large powers, which are not easily accessible in experiments. Moreover, the injection of powerful sidebands may lead to irregular behavior, and seemingly chaotic behavior, dictated by the high sensitivity to initial conditions around a separatrix [23]. Thus, as we did in previous experiments [5,21,22], the power of the sidebands was adjusted in order to excite regular lowest order solutions and at the same time to generate several recurrences. The relative phase between the input wave was modified to control the excitation of these two regimes.

Firstly, the input phase, is set to $\Delta\Phi_{init} = -\pi/2$. This allows to select the regime described by phase-shifted recurrences [16]. In Fig. 2(a), the power evolutions along the fiber length are represented in blue solid line for the pump and red solid line for the signal, respectively. In the first stage, the signal is exponentially amplified until reaching a maximum power level at about 2.4 km while the pump is progressively depleted over this distance. At this stage, the energy transfer is reversed and the signal power is reduced to reach a minimum value at about 4.5 km almost identical to its initial value (0.075 at 4.5 km against 0.085 at the fiber input). This corresponds to the first recurrence. By further propagating within the fiber, the same scenario reproduces itself three more times, leading to the formation of almost four complete recurrences at the fiber output. For each recurrence, the spatial location of the maxima of the pump power coincides well with the minima of the signal power, as expected from theory. These results are validated with numerical simulations achieved by integrating the lossless nonlinear Schrödinger

Optics EXPRESS

equation (NLSE) [15]. They are reported as dotted lines in Fig. 2. It is remarkable that both the position and the amplitude of the extrema of the pump and signal waves from experimental recordings along the fiber are in good agreement with the numerics. Moreover, the values of the pump maxima decrease only slightly along the fiber from 0.83 (first maximum) to 0.73 (fourth maximum). We remind that without loss compensation the overall losses amount to 2.7 dB which corresponds to an attenuation factor of 0.54 for the pump power at the fiber output. This highlights the key role played by the active loss compensation system that we implemented in the experiment. The relative phase evolution is depicted in Fig. 2(b). As shown, the phase is free running, increasing monotonically with much faster variations across the points of maximum depletion corresponding to maximum temporal compression stages. Noteworthy, the phase shows a variation of across each recurrence or across two points of maximum depletion. This means that the phase returns to its initial value (modulus 2π) only after a pair of recurrences. In other words, when also the phase is properly considered the spatial period of the evolution is twice the recurrence distance. The agreement with numerical simulations (grey dotted lines) is excellent. Finally, the evolution of the system is represented in a phase plane in Fig. 2(c) in order to confirm the broken symmetry nature of the recurrence. The curve describing the dynamics of the system spans first the right semi-plane of the phase plane and then extend to the left semi-plane, confirming the symmetry-breaking nature of the recurrence, in agreement with theoretical predictions for this initial phase value [16].

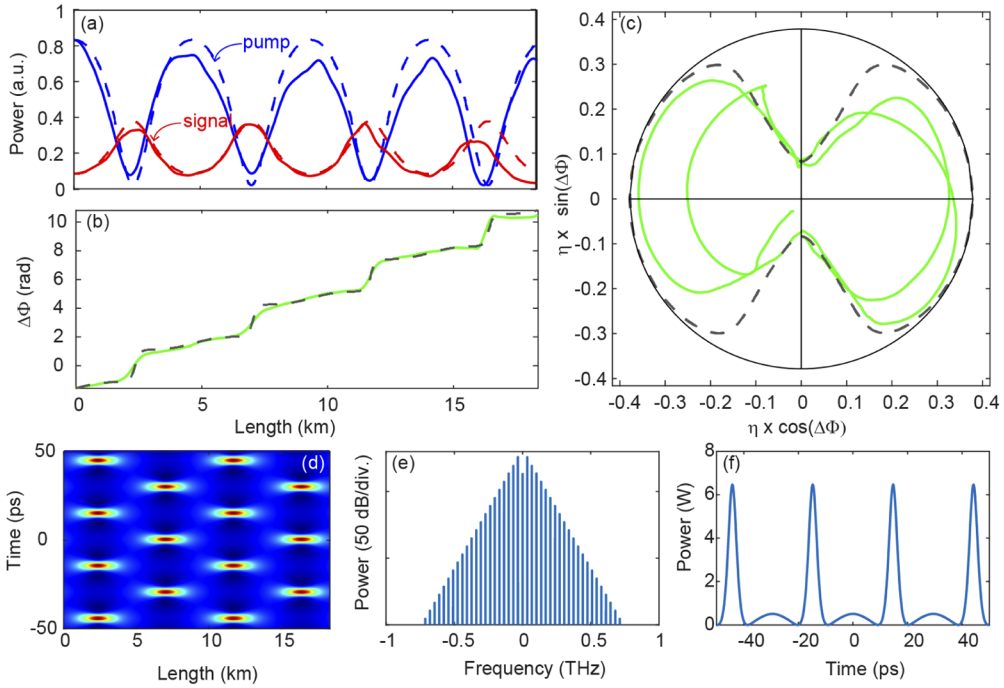

Fig. 2. Longitudinal evolution of (a) the pump (blue line) and signal/idler (red line) powers and (b) their relative phase for $\Delta\Phi_{init} = -\pi/2$; (c) Phase-plane representation. Here η is the signal power normalized to the total power. Solid and dashed lines stand for experimental results and numerical simulations from NLSE, respectively. Bottom line: Numerical results showing (d) spatio-temporal evolution of the power along the fiber length; (e) Spectral and (f) temporal profiles at the first compression point.

The π-shift between two successive maximum compression points is equivalent to a shift of half period in time domain, as explicitly shown in the spatio-temporal evolution of the power

Optics EXPRESS

reported in Fig. 2(d), and obtained from numerical integration of the NLSE. For reference, we also report the relative triangular spectrum and the temporal profile at the first compression stage. We point out that, the reconstruction of the temporal evolution in the experiment would require the measurement of higher-order sidebands [21], which is not carried out with the present setup.

In a second set of measurements, we set the input phase to $\Delta\Phi_{\text{init}} = 0$ to observe regular (unshifted) recurrences. All other parameters are identical to those used in the previous case. The results are displayed in Fig. 3. The first important feature is that five maximum depletion points (or maximally amplified sidebands), in turn corresponding to nearly four and a half recurrences over the same fiber length, are observed. Hence, this case exhibits an excess of nearly half recurrence compared with the previous configuration (see Fig. 3(a)). This is in good agreement with the numerical simulations (see dashed lines in Fig. 3). Moreover, also in this regime, we observe that the spatial location of the extrema of the pump and the signal nearly coincide. The most striking difference with previous case is the boundedness of the phase evolution shown in Fig. 3(b). At variance with the previous case, in Fig. 3(b) the phase exhibits nonlinear oscillations around the input value, not exceeding maximal variation of $\pm\pi/2$.

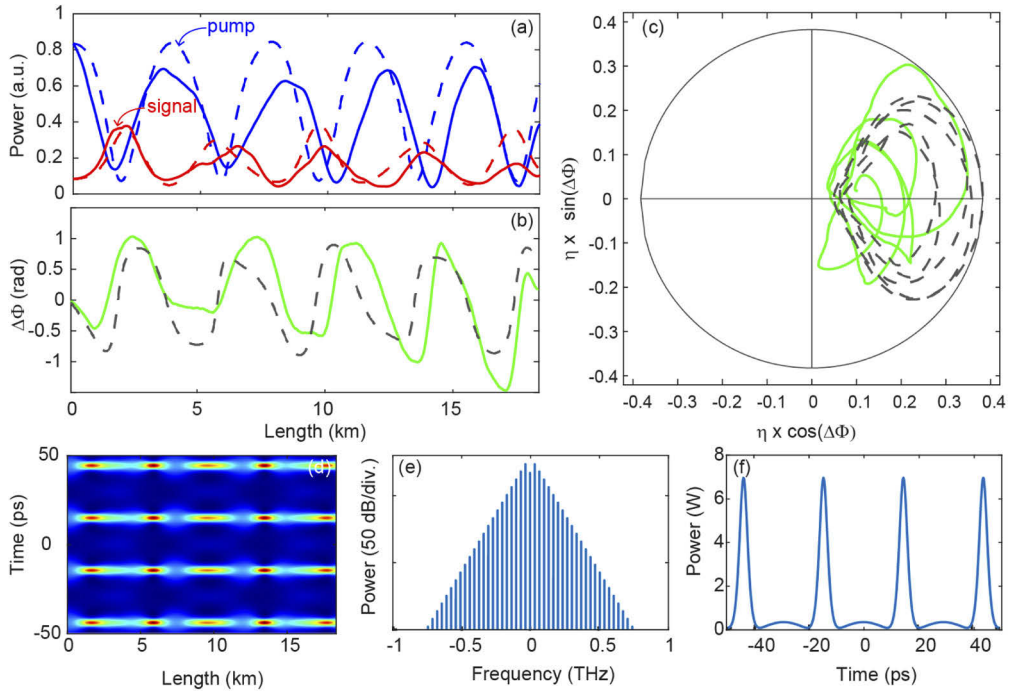

Fig. 3. Same as in Fig. 2 with $\Delta\Phi_{init} = 0$.

In this case, the spatial period coincides with the recurrence distance. The reversals of the direction of energy exchanges correspond to the changes of sign of the phase. The overall dynamics of Fourier modes is summarized in the phase plane displayed in Fig. 3(c). As shown, the trajectory remains confined in the right semi-plane as a consequence of the bounded oscillating phase, in agreement with the expectation from theory for this value of input phase [17]. Importantly, the fact that this curve remains bounded over a semi-plane highlights once again the efficiency of the active loss compensation. Indeed if the system was not almost perfectly conservative, the dissipation could qualitatively modify the nature of the recurrences possibly forcing it to switch from a regular to π-shifted recurrences (see discussion in Ref. [15–16]). The spatio-temporal pattern obtained numerically and displayed in Fig. 3 confirms that no shift is

Optics EXPRESS

experienced in this system and that the maximally compressed trains were indeed formed at five locations along the fiber. It is important to note that the agreement with numerical simulations (dotted lines) is not as good as in the previous case. This is connected to the fact that the inner orbits are less robust and more sensitive to noise and environmental perturbations compared with outer (phase shifted) orbits, as our simulations suggest. In particular, at the level of sideband power of the experiment (which, by the way, is necessary to induce several recurrences over such fiber length), the evolution presents significant deviations from perfectly periodic evolutions that are numerically observed in the noise-less case for sufficiently weak modulations (i.e. signal power below −20 dB). This phenomenon can be also evinced by comparing Fig. 2(d) and Fig. 3(d). In Fig. 2, the repeated leitmotiv in the spatio-temporal representation looks very similar from one recurrence to another. Conversely, as shown in Fig. 3(d), the longitudinal evolution around the third maximum compression point occurring at about 10 km exhibits some features (before and after the peak) that makes it significantly different from the evolutions around the other peak conversion points. This indicates that the system does not evolve in a strictly spatially periodic fashion, but is rather following quasi-periodic orbits in the infinite dimensional space that might be closer to a higher-order solution of the NLSE [23]. A deeper and rigorous analysis is required to exactly identify what type of full solution and the relative order that one is expected to excite by means of the truncated three-wave input condition, as it was done in the context of Akhmediev breathers [24]. This is a challenging issue, definitely out of the scope of the present paper which aims at demonstrating the experimental accessibility of a regime characterized by more than four FPUT recurrences of two different qualitative types along an optical fiber. Finally, we emphasize that, in our experiment, the system is found to undergo four or more regular cycles of conversion and back-conversion without showing the strong departures that characterize the onset of thermalization, as discussed in Ref. [13], and numerically estimated to appear after very few cycles of recurrences. Clearly, we expect the noise level to have a central role in the onset of thermalization, which, in our system, we believe to occur at longer distances, unfortunately not accessible with the present set-up.

4. Conclusions

We reported the observation of four Fermi-Pasta-Ulam-Tsingou recurrences in an optical fiber by employing an ultra-low loss optical fiber and an active compensation of the losses. We obtained a pretty good agreement with numerical simulations based on the lossless NLSE confirming the efficiency of the active loss compensation scheme that we implemented by using a counter-propagating Raman pump. These results open the way to investigate further complex problems such as the role of multiple unstable sideband pairs and the route to the thermalization using longer fiber spans, following the inspiration from the original work by Fermi, Pasta, Ulam and Tsingou, which, though widely investigated in theory, is rarely addressed in real experiments. In order to extend the measurements to longer fiber lengths and possibly explore the thermalization stage, we envisage to improve further the Raman amplification system, also considering the use of dual Raman pump injected in both the co-propagating and counter-propagating directions [25]. The recirculating loops also employed in [7] represents a valid alternative to reach extremely long distances, which can be combined with lumped or partially distributed amplification [26], though, in this case, the unavoidable periodic output coupling represents a significant deviation from the ideally lossless situation described by the integrable model considered here.

Funding

Agence Nationale de la Recherche (CPER P4S, EXAT, FUHNCK, PIA).

Optics EXPRESS

Acknowledgments

This work was partly supported by the Agence Nationale de la Recherche through the "Programme Investissements d'Avenir," by the Ministry of Higher Education and Research, Hauts de France Council and European Regional Development Fund (ERDF) through the Contrat de Projets Etat-Region (CPER Photonics for Society, P4S) project and SITE ULNE through the FUHNKC and EXAT projects.

Disclosures

The authors declare no conflicts of interest.

References

1. E. Fermi, J. Pasta, and S. Ulam, in *Collected Papers of Enrico Fermi* (ed. E. Segre), pp. 978–988 (University of Chicago Press, 1965).
2. B. M. Lake, H. C. Yuen, H. Rungaldier, and W. E. Ferguson, "Nonlinear deep-water waves: theory and experiment. Part 2. Evolution of a continuous wave train"," J. Fluid Mech. **83**(1), 49–74 (1977).
3. G. Van Simaeys, P. Emplit, and M. Haelterman, "Experimental Demonstration of the Fermi-Pasta-Ulam Recurrence in a Modulationally Unstable Optical Wave," Phys. Rev. Lett. **87**(3), 033902 (2001).
4. A. Mussot, A. Kudlinski, M. Droques, P. Szriftgiser, and N. Akhmediev, "Fermi-Pasta-Ulam Recurrence in Nonlinear Fiber Optics: The Role of Reversible and Irreversible Losses," Phys. Rev. X **4**(1), 011054 (2014).
5. A. Mussot, C. Naveau, M. Conforti, A. Kudlinski, F. Copie, P. Szriftgiser, and S. Trillo, "Fibre multi-wave mixing combs reveal the broken symmetry of Fermi–Pasta–Ulam recurrence," Nat. Photonics **12**(5), 303–308 (2018).
6. X. Hu, W. Chen, Y. Lu, Z. Yu, M. Chen, and Z. Meng, "Distributed Measurement of Fermi–Pasta–Ulam Recurrence in Optical Fibers," IEEE Photonics Technol. Lett. **30**(1), 47–50 (2018).
7. J.-W. Goossens, H. Hafermann, and Y. Jaouën, "Experimental realization of Fermi-Pasta-Ulam-Tsingou recurrence in a long-haul optical fiber transmission system," Sci. Rep. **9**(1), 1–11 (2019).
8. D. Pierangeli, M. Flammini, L. Zhang, G. Marcucci, A. Agranat, P. G. Grinevich, P. M. Santini, C. Conti, and E. Del Re, "Observation of Fermi-Pasta-Ulam-Tsingou Recurrence and Its Exact Dynamics," Phys. Rev. X **8**(4), 041017 (2018).
9. N. J. Zabusky and M. D. Kruskal, "Interaction of solitons in a collisionless plasma and the recurrence of initial states," Phys. Rev. Lett. **15**(6), 240–243 (1965).
10. D. Jäger, "Soliton propagation along periodic-loaded transmission line," Appl. Phys. **16**(1), 5–38 (1978).
11. S. Trillo, G. Deng, G. Biondini, M. Klein, G. Clauss, A. Chabchoub, and M. Onorato, "Experimental Observation and Theoretical Description of Multisoliton Fission in Shallow Water"," Phys. Rev. Lett. **117**(14), 144102 (2016).
12. Y. V. Lvov and M. Onorato, "Double Scaling in the Relaxation Time in the beta-Fermi-Pasta-Ulam-Tsingou Model," Phys. Rev. Lett. **120**(14), 144301 (2018).
13. S. Wabnitz and B. Wetzel, "Instability and noise-induced thermalization of Fermi-Pasta-Ulam recurrence in the nonlinear Schrödinger equation," Phys. Lett. A **378**(37), 2750–2756 (2014).
14. Y. Tamura, H. Sakuma, K. Morita, M. Suzuki, Y. Yamamoto, K. Shimada, Y. Honma, K. Sohma, T. Fujii, and T. Hasegawa, ""The First 0.14-dB/km Loss Optical Fiber and its Impact on Submarine Transmission", J. Lightwave Technol.," J. Lightwave Technol. **36**(1), 44–49 (2018).
15. B. Kibler, "Rogue Breather Structures in Nonlinear Systems with an Emphasis on Optical Fibers as Testbeds," in *Shaping Light in nonlinear optical fibers*, S. Boscolo and C. Finot, eds. (Wiley, New York, 2017).
16. O. Kimmoun, H. C. Hsu, H. Branger, M. S. Li, Y. Y. Chen, C. Kharif, M. Onorato, E. J. R. Kelleher, B. Kibler, and N. Akhmediev, "Modulation Instability and Phase-Shifted Fermi-Pasta-Ulam Recurrence," Sci. Rep. **6**(1), 28516 (2016).
17. S. Trillo and S. Wabnitz, "Dynamics of the nonlinear modulational instability in optical fibers," Opt. Lett. **16**(13), 986–988 (1991).
18. H. T. Moon, "Homoclinic crossings and pattern selection," Phys. Rev. Lett. **64**(4), 412–414 (1990).
19. N. N. Akhmediev, V. M. Eleonskii, and N. E. Kulagin, "Exact first-order solutions of the nonlinear Schrödinger equation," Theor. Math. Phys. **72**(2), 809–818 (1987).
20. M. Conforti, A. Mussot, A. Kudkinski, S. Trillo, and N. Akhmediev, "Doubly-periodic solutions of the focusing nonlinear Schrödinger equation: recurrence, period doubling, and amplification outside the conventional modulational instability band," Phys. Rev. A **101**(2), 023843 (2020).
21. C. Naveau, P. Szriftgiser, A. Kudlinski, M. Conforti, S. Trillo, and A. Mussot, "Full-field characterization of breather dynamics over the whole length of an optical fiber," Opt. Lett. **44**(4), 763–766 (2019).
22. C. Naveau, P. Szriftgiser, A. Kudlinski, M. Conforti, S. Trillo, and A. Mussot, "Experimental characterization of recurrences and separatrix crossing in modulational instability," Opt. Lett. **44**(22), 5426–5429 (2019).
23. B. M. Herbst and M. J. Ablowitz, "Numerically induced chaos in the nonlinear Schrödinger equation," Phys. Rev. Lett. **62**(18), 2065–2068 (1989).
24. M. Erkintalo, G. Genty, B. Wetzel, and J. M. Dudley, "Akhmediev breather evolution in optical fiber for realistic initial conditions," Phys. Lett. A **375**(19), 2029–2034 (2011).

Optics EXPRESS

25. J. D. Ania-Castanon, T. J. Ellingham, R. Ibbotson, X. Chen, L. Zhang, and S. K. Turitsyn, "Ultralong Raman fiber lasers as virtually lossless optical media," Phys. Rev. Lett. **96**(2), 023902 (2006).
26. A. E. Kraych, D. Agafontsev, S. Randoux, and P. Suret, "Statistical Properties of the Nonlinear Stage of Modulation Instability in Fiber Optics," Phys. Rev. Lett. **123**(9), 093902 (2019).